Astron. Astrophys. 338, 713–722 (1998)

ASTRONOMY
AND
ASTROPHYSICS

Sulphur chemistry and evolution in hot cores

J. Hatchell[1], **M.A. Thompson**[2], **T.J. Millar**[1], **and G.H. Macdonald**[2]

[1] Department of Physics, UMIST, P.O. Box 88, Manchester M60 1QD, UK
[2] Electronic Engineering Laboratory, University of Kent, Canterbury, Kent CT2 7NT, UK

Received 5 June 1998 / Accepted 20 July 1998

Abstract. We compare the results of our JCMT spectral line survey of molecular gas towards ultracompact HII regions with the predictions of models of sulphur chemistry in hot cores. We investigate the range of evolutionary models that are consistent with the observed physical conditions and chemical abundances, and see to what extent it is possible to constrain core ages by comparing abundances with the predictions of chemical models. The observed abundance ratios vary little from source to source, suggesting that all the sources are at a similar evolutionary stage. The models are capable of predicting the observed abundances of H_2S, SO, SO_2, and CS. The models fail to predict the amount of OCS observed, suggesting that an alternative formation route is required. An initial H_2S abundance from grain mantle evaporation of $\sim 10^{-7}$ is preferred.

Key words: ISM: molecules – ISM: clouds – ISM: HII regions – molecular processes – radio lines: ISM

1. Introduction

Hot cores have a rich and unique chemistry. Unlike cold dense clouds, hot cores have high densities of saturated molecules such as NH_3 and H_2O. These molecules are believed to form in icy mantles on dust grains, created from constituents deposited during the high density phases of collapse. As the cores heat up in the star formation process, the grain mantles are evaporated and the mantle species are released into the gas phase. At the high temperatures and densities of hot cores, the chemistry evolves rapidly, transforming many of the grain mantle products into daughter species on timescales of less than 100,000 years.

It has been suggested that molecular abundances in hot cores can be used as chemical clocks, measuring the time elapsed since the onset of core heating. This method was used with some success in W3 (Helmich et al. 1994). Charnley (1993) proposed that sulphur chemistry might be particularly useful as a tracer of evolution, and has published a detailed study of the chemical network for sulphur-bearing molecules, predicting the time evolution and comparing with observations of the Orion Hot Core, the Orion Compact Ridge, and Sgr B2N (Charnley 1997). Because of the relatively rapid evolution of the chemistry, sulphur-bearing species are particularly good candidates for tracing evolution in hot cores. During the cold collapse phase, sulphur freezes out onto grains and remains there in the form of H_2S until core heating begins. At this point, H_2S is evaporated from the grains, and rapidly undergoes reactions which drive the production of SO and SO_2. Unlike nitrogen chemistry or oxygen chemistry, most of the molecules involved are easy to detect at mm and submm wavelengths and column densities can be calculated easily. Although other species such as CH_3OH and NH_3 can also be used to constrain the evolutionary timescales, sulphuretted species have the most potential as chemical clocks.

In this paper we aim to identify evolutionary models of sulphur chemistry which are consistent with the physical conditions and observationally-determined column densities in a sample of hot cores associated with ultracompact HII regions, and to see to what extent it is possible to constrain core ages by comparing abundances with the predictions of the evolutionary models. The elements required for this study are: a chemical model which can be tailored to the physical conditions in hot cores; abundance estimates for a variety of species which can be compared with the models; and thirdly, estimates of the physical conditions appropriate to the hot cores for which we have abundance estimates.

We have recently carried out a molecular line survey of hot cores (Hatchell et al. 1998b, hereafter 'the survey paper'), from which we draw the majority of our abundance estimates. In the survey paper we reported detections of many species, including a number of sulphur species, in a sample of 14 hot cores. We consider here only the 8 sources listed in Table 1 in which several sulphur species other than $C^{34}S$ were detected. Additional serendipitous detections of sulphur species lines in more recent observations of hot cores have enabled us to enlarge the list of species and further constrain the column densities. Information on the physical conditions in the cores, which is needed in order to produce appropriate chemical models, is also taken from the survey paper.

The chemical model we use is based on the model of hot core chemistry developed by Millar et al. (1997). This model, which was tailored to the physical and chemical conditions of G34.26, calculated the abundances of over 200 species as a function of time and depth in the core. Here we use the same chemical

Send offprint requests to: J. Hatchell

network to follow the sulphur chemistry. As we are not sure of the variations in source size and structure between the cores studied, we are not integrating over the series of shells used by Millar et al. (1997), but instead consider regions characterised by a single temperature and density, which are varied to explore a range of different physical conditions appropriate to hot cores, rather than halo gas.

In the following section (Sect. 2) we briefly describe the new observations. Sect. 3 covers the results of our hot core chemical model for the evolution of sulphur-bearing molecules, and the abundances calculated from observation. In Sect. 4 we compare the model's predictions with the observational results.

2. Observations

The original observations for the hot cores survey were made in September 1995 and April 1996 using the James Clerk Maxwell telescope (JCMT)[1]. The details of these observations have already been reported in Hatchell et al. 1998b. Additional detections of sulphur bearing species were made serendipitously in May 1997, also using the JCMT, during observations of DCN and HCN, SiO and CH_3OH, the results of which will appear elsewhere (Hatchell et al. 1998a and subsequent publications). These further observations used the common-user receivers A2 (230 GHz band) and B3 (345 GHz band) coupled to the DAS (Dutch Autocorrelation Spectrometer). The bandwidth was a nominal 760 MHz, giving a frequency resolution of 0.756 MHz. Each spectrum was divided into channels of width 0.625 MHz. Dual sideband mode was used for most of the observations. In the 230 GHz band, sidebands were centred ± 3 GHz from the main band. In the 345 GHz band, sidebands were separated by ± 8 GHz. To resolve sideband ambiguities observations were repeated with the line of interest centred first in the upper and then the lower sideband. In some cases we changed the local oscillator frequency by 10 MHz to shift the image sideband lines relative to the main band lines. Single sideband spectra were taken at 338 GHz with a sideband rejection of about a factor of 20. Pointing was checked on G34.26 and W75N and was accurate to within $5''$ throughout the observations. System temperatures were typically in the range 300–1000 K with RxA2 and 500 K-1500 K with RxB3. Line brightness temperatures have been corrected for telescope main beam efficiency $\eta_{\rm MB}$ and are given as $T_{\rm R}^*$ in kelvin. $\eta_{\rm MB}$ was 0.8 for receiver A2 and 0.6 for receiver B3. THe JCMT beam FWHM is $21''$ at 230 GHz and $14''$ at 345 GHz. Integrated intensities for ^{34}SO and C^{34}S in G5.89 are from the 330-360 GHz survey of this source; these observations will be reported in full by Thompson & Macdonald (1998).

The observed sources are listed in Table 1 with the positions, distances (Churchwell et al. 1990), and LSR velocities (from ammonia; Cesaroni et al. 1992, Olmi et al. 1993) assumed.

[1] The James Clerk Maxwell Telescope is operated by The Joint Astronomy Centre on behalf of the Particle Physics and Astronomy Research Council of the United Kingdom, the Netherlands Organisation for Scientific Research, and the National Research Council of Canada.

Table 1. Positions, velocities and distances for observed objects

Object	α_{1950} [h m s]	δ_{1950} [° ′ ″]	$v_{\rm LSR}$ [kms^{-1}]	d [kpc]
G5.89−0.39	17 57 26.8	−24 03 56	9.0	2.5
G9.62+0.19	18 03 16.2	−20 32 03	4.4	5.7
G10.47+0.03	18 05 40.3	−19 52 21	67.8	5.8
G12.21−0.10	18 09 43.7	−18 25 09	24.0	13.5
G29.96−0.02	18 43 27.1	−02 42 36	97.6	7.4
G31.41+0.31	18 44 59.4	−01 16 04	97.4	7.9
G34.26+0.15	18 50 46.1	01 11 12	58.0	4.0
G75.78+0.34	20 19 52.0	37 17 02	−0.1	4.1

3. Results

3.1. Observed abundances

Integrated intensities for detected lines are given in Table 2. These results are taken from the survey paper, with the exception of OCS and H_2CS (which were detected only during the second set of observations) and SO and SO_2, for which we added more line detections during 1997. The extra lines detected for SO and SO_2 enable us to produce rotation diagrams for these species in a number of sources, estimating both rotation temperature and column density (see survey paper for method). For the other molecules, we estimate column density lower limits using Eq. 5 of the survey paper. The resulting beam-averaged column densities for detected sulphur bearing species are given in Table 3.

The column density estimates for H_2S, H_2CS, SO, SO_2 and OCS are plotted in Fig. 1. These species, linked by the network described in the previous section, provide our main tests of the chemical models. The remaining sulphur-bearing molecules observed, HDS, SiS and NS, form links between the sulphur/carbon/oxygen chemistry and deuterium, silicon and nitrogen chemistries respectively.

To compare with models, it is useful to convert the observed column densities into abundances. This is not straightforward as the molecular hydrogen column density $N_{\rm H_2}$ varies with radius, increasing towards the core centres, and it is necessary to make an assumption about the location and extent of the sulphur species emission. In the survey paper we made estimates of the H_2 column density in the outer halo, traced by CO, by assuming a fixed H_2/CO ratio; and in the core, from combining the size of the CH_3OH emitting region with its virial mass. These H_2 column density estimates are also plotted in Fig. 1. In order to account for the small size of the core, the H_2 column densities from CH_3OH are given as an average over a $22''$ beam, assuming the source sizes given in the survey paper (which range from 1-5$''$). The beam-averaged H_2 column densities from the core are typically an order of magnitude lower than those from the halo, corresponding to a true core column density an order of magnitude higher than in the halo diluted by a beam filling factor of 20-400.

Abundances of H_2S, H_2CS, SO, SO_2, OCS and CS (from C^{34}S, using C^{32}S/C^{34}S = 20) compared to the beam-averaged

Table 2. Integrated intensities. An 'x' denotes a non-detection; a dash indicates that no observation was made at this frequency.

Line	ν / GHz	$E_{\rm U}$ / K	Integrated intensity / K MHz							
			G5.89	G9.62	G10.47	G12.21	G29.96	G31.41	G34.26	G75.78
H_2S	216.710	84.0	-	7.7	20.0	-	6.3	7.5	18.0	1.6
OCS	255.374	134.8	5.05	3.70	14.1	2.46	3.04	4.18	12.1	0.94
H_2CS	338.080	102.5	23.2	17.0	30.6	10.7	7.5	8.7	31.1	2.1
$C^{34}S$	337.397	64.8	4.7	17.7	2.36	12.0	9.86	30.1	68.2	5.13
SO_2	216.643	248.5	-	0.41	3.70	-	0.54	1.05	4.74	0.75
SO_2	238.993	332.5	-	-	-	-	-	-	3.61	-
SO_2	255.553	31.3	11.8	x	x	x	x	7.84	4.98	2.65
SO_2	258.389	531.1	-	-	3.47	-	-	-	1.84	-
SO_2	338.305	196.8	25.5	x	10.7	1.18	1.67	x	9.90	1.63
SO_2	346.652	168.1	-	1.50	3.84	1.91	3.10	1.87	14.2	7.01
SO_2	355.045	111.0	-	2.94	38.0	-	4.04	8.57	19.6	-
$^{34}SO_2$	338.320	92.5	8.06	x	x	x	x	x	x	x
$^{34}SO_2$	338.785	134.3	6.73	x	x	x	x	x	2.15	x
SO	219.949	78.8	-	12.9	11.2	11.2	8.02	12.1	49.2	26.3
SO	258.255	56.5	-	8.57	12.6	-	8.32	-	-	13.1
SO	346.529	35.0	-	9.36	11.8	8.47	6.64	6.16	20.9	11.3
^{34}SO	333.902	79.9	1.87	x	4.32	x	x	2.18	8.22	1.69
HDS	257.781	47.0	x	2.52	x	-	x	1.67	-	x
SiS	235.961	79.3	-	0.97	3.91	2.50	0.23	4.03	4.52	0.15
NS	346.221	94.8	-	3.40	4.85	2.63	3.97	3.12	13.7	1.16

Table 3. Column density lower limits. For SO and SO_2, lower limits (limit) from ^{32}SO and $^{32}SO_2$ and estimates from rotation diagrams (r.d.) are listed along with the rotation temperatures $T_{\rm rot}$ in kelvin. For SO, SO_2 and CS, lower limits from ^{34}SO and $^{34}SO_2$ multiplied by $^{32}S/^{34}S \simeq 20$ are also listed.

Line	Column density / 10^{14}cm^{-2}							
	G5.89	G9.62	G10.47	G12.21	G29.96	G31.41	G34.26	G75.78
H_2S	-	> 3.78	> 10.6	-	> 4.51	> 2.69	> 4.38	> 0.87
OCS	> 3.26	> 2.39	> 9.10	> 1.59	> 1.96	> 2.70	> 7.81	> 0.61
H_2CS	> 0.67	> 0.50	> 0.89	> 0.31	> 0.22	> 0.25	> 0.91	> 0.06
$C^{34}S$	> 0.19	> 0.18	> 0.24	> 0.13	> 0.21	> 0.31	> 0.71	> 0.05
$C^{34}S\times20$	> 3.8	> 3.6	> 4.8	> 2.6	> 4.2	> 6.2	> 14.2	> 1.0
SO_2 (limit)	> 5.89	> 0.59	> 6.60	> 0.27	> 0.78	> 2.18	> 3.27	> 1.47
SO_2 (r.d.)	-	4.7 ± 1.8	33 ± 12	-	6.8 ± 0.9	9.2 ± 3.1	30 ± 9	-
($T_{\rm rot}$ /K)	-	(167 ± 129)	(139 ± 58)	-	(136 ± 29)	(174 ± 146)	(198 ± 103)	-
$^{34}SO_2$	> 1.71	x	x	x	x	x	> 0.20	x
$^{34}SO_2 \times 20$	> 34.2	x	x	x	x	x	> 4.0	x
SO (limit)	-	> 2.17	> 2.99	> 0.37	> 1.46	> 2.01	> 4.57	> 2.39
SO (r.d.)	-	-	2.2 ± 0.7	-	1.3 ± 0.4	-	-	3.0 ± 0.2
($T_{\rm rot}$ / K)	-	-	(32 ± 12)	-	(39 ± 19)	-	-	(92 ± 18)
^{34}SO	> 0.47	x	> 0.29	x	x	> 0.15	> 0.56	> 0.12
$^{34}SO\times20$	> 9.4	x	> 5.8	x	x	> 3.0	> 11.2	> 2.4
HDS	x	> 0.20	x	-	x	> 0.14	-	x
SiS	-	> 0.09	> 0.38	> 0.24	> 0.02	> 0.39	> 0.44	> 0.01
NS	-	> 0.37	> 0.52	> 0.28	> 0.43	> 0.33	> 1.47	> 0.12

'core' H_2 column density are plotted in Fig. 2. If the emission is from the halo, then abundances are about an order of magnitude less. Relative to the core, the abundances of H_2S and OCS range from 10^{-9} to 10^{-8} and those of H_2CS from 10^{-10} to 1×10^{-9}. SO and SO_2 show slightly more variation between sources with abundances from 5×10^{-10} to 2×10^{-8}. There is less variation in

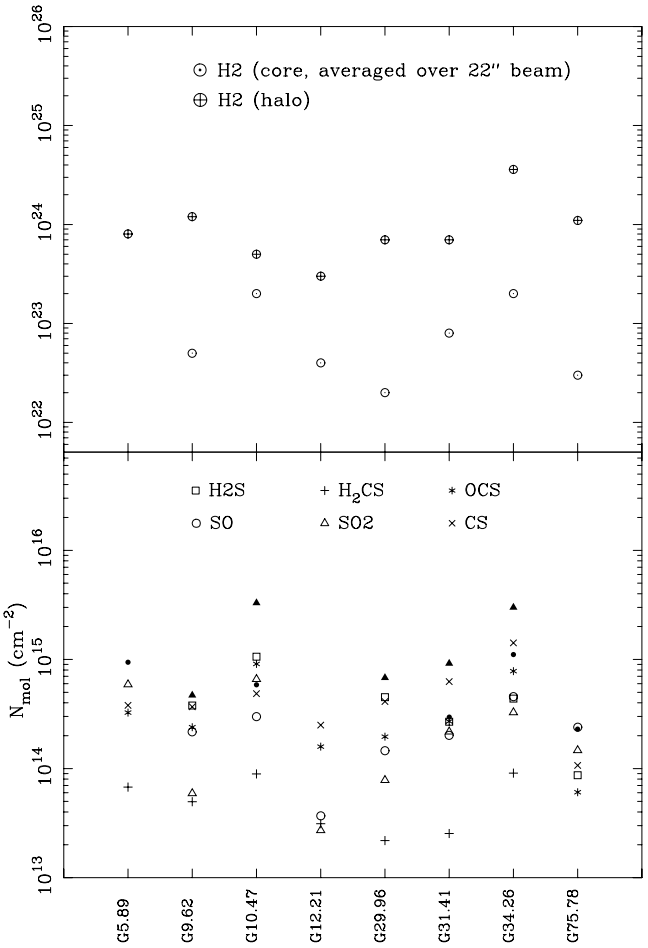

Fig. 1. Column densities of H_2S, H_2CS, SO, SO_2, CS and OCS for each source (bottom) and H_2 column density estimates (top) for the core and halo. For SO, the open circles are lower limits from ^{32}SO and filled circles lower limits from ^{34}SO. For SO_2, the open triangles are column density lower limits from $^{32}SO_2$ and filled triangles are estimates from rotation diagrams.

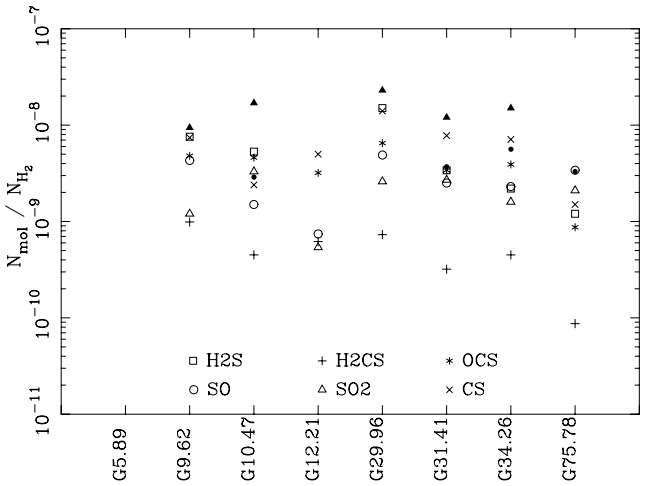

Fig. 2. Abundances of H_2S, H_2CS, SO, SO_2, CS and OCS for each source relative to H_2 estimates for the core.

abundance than in column density, with the column densities of the sulphur species tracking the H_2 column densities estimated for the core (Fig. 1). Abundance variations can be seen more clearly in Fig. 3, in which the abundances are plotted relative to CS.

3.2. Modelling

Using a chemical model based on the hot core model developed by Millar et al. (1997), we modelled the chemical evolution of a number of sulphur-bearing molecules for a range of conditions appropriate to hot cores. The results of the modelling are shown in Figs. 4–6.

Briefly, the chemistry proceeds by the destruction of the grain-evaporated H_2S by H and H_3O^+ to produce reactive sulphur in the form of S or H_3S^+, respectively. Reactions primarily with OH and O_2 then produce the daughter products SO and SO_2. H_2S also reacts with C^+ and this leads to the formation of CS. OCS is formed by reaction of CO and atomic sulphur, and H_2CS by reaction of CH_3 and atomic sulphur.

The evaporation of H_2S from grains is represented by the high initial H_2S abundance at early times in the models. The SO and SO_2 abundances increase with time, peaking after a substantial fraction of the injected H_2S has been destroyed. At large times, SO and SO_2 reduce to a small fraction of their peak abundances, and most of the sulphur is found in the form of CS, H_2CS and OCS.

For full details of the reaction network, see Charnley (1997) and Millar et al. (1997). Charnley (1997) describes in detail a sulphur chemistry which is essentially the same as that used here. One small difference is that we use an updated rate for the reaction of H_2S with atomic hydrogen. We are using a lower energy barrier of $E_A \simeq 350$ K, following Yoshimura et al. (1989), rather than the $E_A \sim 850$ K barrier of Leen & Graff (1988) used in the UMIST RATE91 database (Millar et al. 1991) and by Charnley (1997). However, between 200 and 450 K the models predict essentially the same rate. If we match our physical conditions and initial abundances to those used by Charnley (1997) the resulting evolution is essentially the same.

The chemical initial conditions for the model are as follows. The grain-evaporated species are given initial abundances as if they were simultaneously released into the gas phase from the grain ices. No grain chemistry is included so these initial abundances are estimates from observations of ices and molecules in the gas phase. The initial abundance of H_2S is taken to be 10^{-6} in all models, following measurements in Orion (Minh et al. 1990); the subsequent abundances of the other sulphur species more or less scale with this value. The initial O_2 abundance can also influence the sulphur chemistry: this is taken to

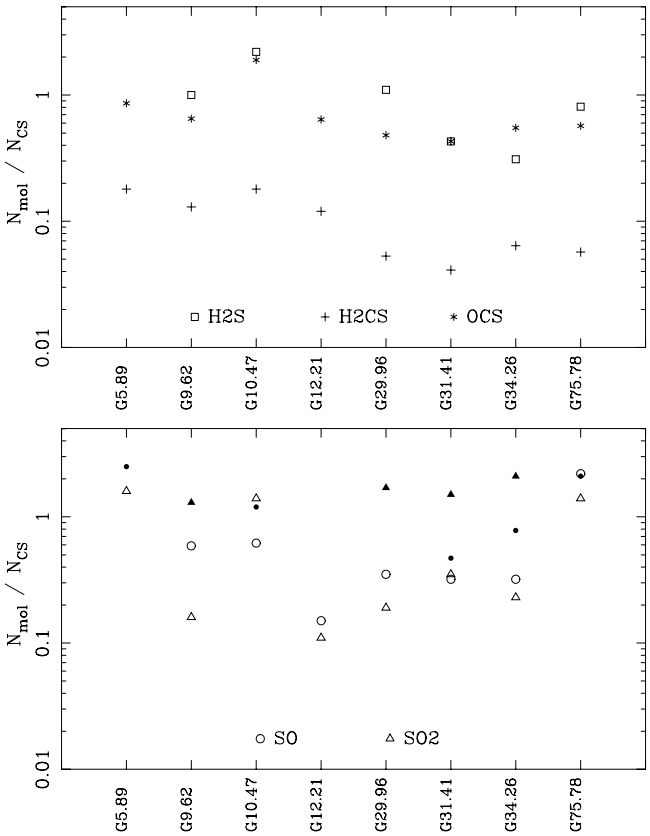

Fig. 3. Abundances of H_2S, H_2CS and OCS (top) and SO and SO_2 (bottom) relative to CS.

be 1×10^{-6} (Charnley 1997). Other initial abundances are as in Millar et al. (1997).

The timescales and the actual abundances predicted by the model vary with temperature, cosmic ray rate and density. We consider gas with densities from 2×10^5 cm^{-3} – 2×10^7 cm^{-3}, temperatures from 50–300 K and take the cosmic ray rate to be either 'standard interstellar' (1.3×10^{-17} s^{-1}), 'enhanced' (1.3×10^{-16} s^{-1}) or 'super enhanced' (1.3×10^{-15} s^{-1}). Millar et al. (1997) found the 'enhanced' cosmic ray rate of 1.3×10^{-16} cm^{-16} to be necessary to explain the high abundance of HCO^+ observed in the haloes of hot cores, so the cosmic ray rates that we consider lie above rather than around the 'standard interstellar' value.

Fig. 4 shows the chemical evolution for the molecules H_2S, SO, SO_2, OCS, and CS, for temperatures of 50 K, 100 K, 200 K and 300 K, with a constant cosmic ray rate of 1.3×10^{-16} s^{-1} and density of 2×10^6 cm^{-3}. Fig. 5 shows the effect of varying the density from 2×10^5 cm^{-3} to 2×10^7 cm^{-3} at 100 K with a cosmic ray rate of 1.3×10^{-16} s^{-1}. Of these variables, the temperature and cosmic ray rate have the greatest effects on the timescales. Density has relatively little effect on the chemistry. Finally, Fig. 6 shows the variation in the evolution with cosmic ray rates increasing from the standard Galactic interstellar value of 1.3×10^{-17} s^{-1} to 1.3×10^{-16} s^{-1} and 1.3×10^{-15} s^{-1}, at 100 K with a density of 2×10^6 cm^{-3}.

The variation of timescales with temperature and cosmic ray rate can be illustrated by looking at two simple indicators: the time at which H_2S is destroyed, and the time at which the SO_2 abundance peaks. Fig. 4 shows that the variation in H_2S drops to 1% of its initial abundance after 4,000 years at 300 K; at 50 K it takes 30,000 years. SO_2 peaks at around 20,000 years or slightly later at 300 K. (The 300 K model is the only one in which SO_2 peaks substantially later than SO). Increasing the cosmic ray rate rapidly increases the rate at which H_2S is processed away: a factor of 100 change in the cosmic ray rate introduces a similar factor in the timescales, with H_2S destruction and SO_2 abundance peaking at 3,000 years for $\zeta = 1.3 \times 10^{-15}$ and 200,000 years for $\zeta = 1.3 \times 10^{-17}$.

4. Discussion

In this section we compare the observations with the models. First we look at whether the models can predict the abundances observed at any time. Second, we look at the timescales and whether we can distinguish sources at different stages of evolution from the chemistry. The main products of the H_2S-driven chemistry are H_2CS, SO, SO_2, CS and OCS and the abundances of these molecules provide our main observational tests.

As a starting point, we take the emission to be from the core rather than the halo. The H_2S line has an excitation energy of 84 K, which requires warm gas to excite, and H_2S abundances of above 10^{-10} are hard to explain without grain mantle evaporation (as are many of the other species detected in these cores). The detected transitions of H_2CS and OCS, which can be produced by cool gas chemistry, cannot be emission from the extended halo because of the high excitation energies, 102 and 135 K, of the lines detected. For SO_2, the estimated rotation temperatures are high, > 100 K, and suggest emission from the core rather than the halo. The high excitation temperatures suggest that emission is coming from a region similar to that with CH_3OH emission (temperature estimates from CH_3OH are 50–70 K), and that the H_2 column density estimates from CH_3OH are appropriate for calculating abundances.

The SO and CS lines are more likely to include a contribution from the halo. The upper state energy of the $C^{34}S$ transition detected is 65 K, suggesting warm rather than cool gas, but CS is widespread in molecular clouds and in cool gas with sufficient density the population in these states could be significant. SO rotation temperatures are low for G10.47 and G31.41 (though not for G75.78), although the 219.95 GHz line which is 79 K above ground is detected in all sources. The low rotation temperatures suggest that halo models may be more appropriate for this molecule; halo chemistry predicts more SO than SO_2 and this may dominate over any warm component (Millar et al. 1997). In G34.26, column densities in the halo (at a $20''$ offset to the north of the core) compared to the core are a factor of 10 less for SO and a factor of 2 for CS, suggesting that CS is dominated by the widespread component but SO is not. However, we continue

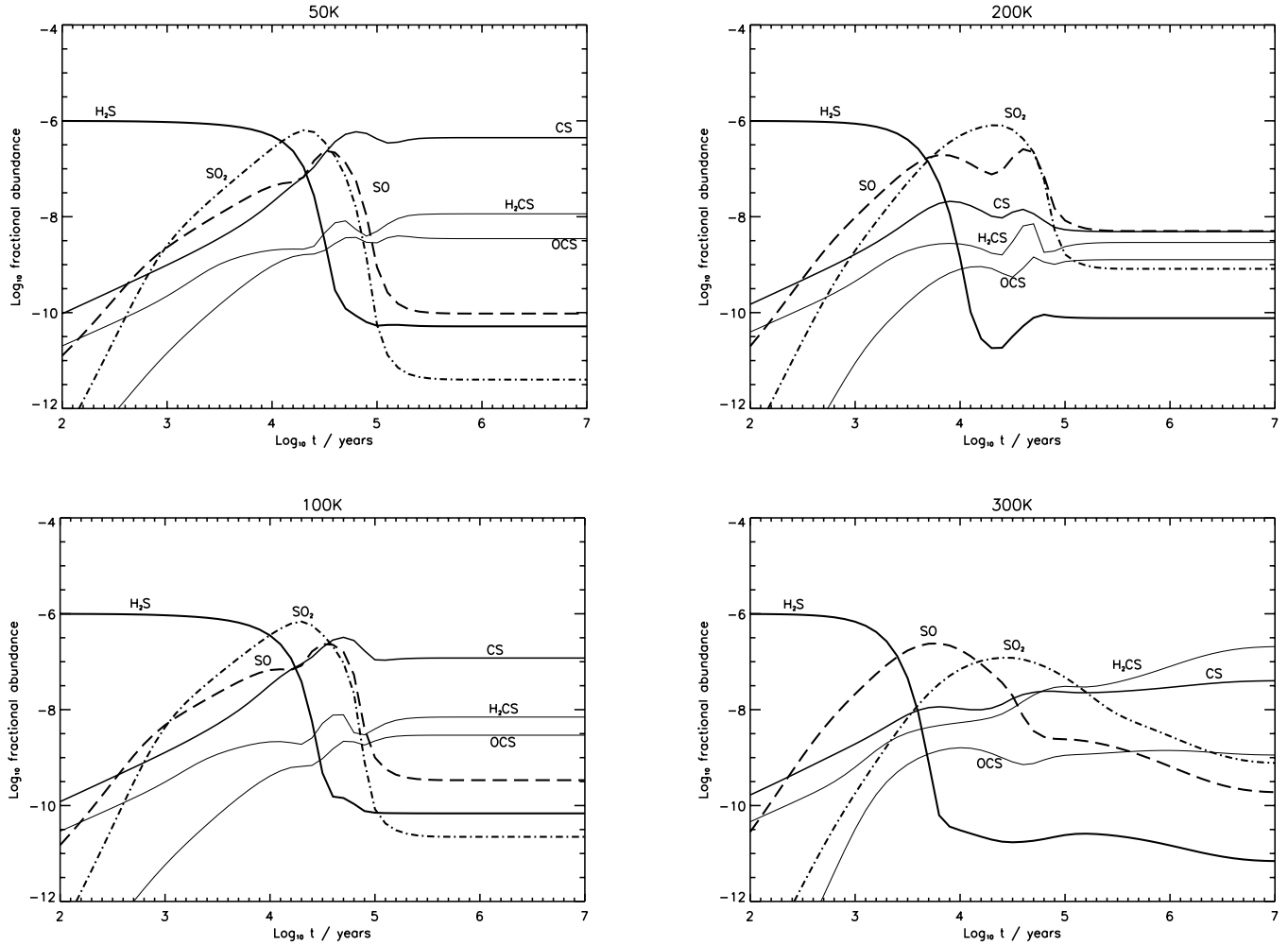

Fig. 4. Evolution of sulphur chemistry for different temperatures ($T_{\rm kin}$ = 50, 100, 200 and 300 K) at a density of $n_{\rm H_2} = 2 \times 10^6$ cm^{-3} and cosmic ray rate of $\zeta = 1.2 \times 10^{-16}$ s^{-1}.

on the assumption that all emission is from the core and see if both SO and CS abundances can be explained in this way.

Comparing the abundance lower limits from Fig. 2 with the models in Figs. 4 – 5, we see that the observed abundances are exceeded for each species for long periods by all the models. The models are quite capable of producing large enough abundances; in fact, the models predict peak abundances significantly above those observed, with peak abundances of 10^{-7}–10^{-6} rather than the observed 10^{-8} predicted for H_2S, SO_2, SO and CS. Although the observed abundances are strictly lower limits, this large discrepancy between model and observations is hard to reconcile. Evidence from ^{34}SO and $^{34}SO_2$, and from rotation diagrams, suggest that the calculated abundances underestimate by at most factor of ten. The models do predict similar abundances of H_2S, SO and SO_2 at certain times, but with abundances of order 10^{-7} rather than 10^{-9}–10^{-8}. There is also a difficulty in producing the abundances of H_2S and OCS, which are observed to be very similar, at the same time. Another problem is H_2CS abundances which are less than an order of magnitude below H_2S, SO and SO_2 abundances in several sources, whereas the models predict differences of two orders of magnitude or more.

None of the models can produce the simultaneous abundances of H_2S, SO and SO_2 of between 10^{-9} and 10^{-8}, which would directly agree with the observations. This may mean that the initial H_2S abundance used in the models, currently set at 10^{-6} from observations in Orion (Minh et al. 1990), is too high. The initial abundance of H_2S injected from the grain mantles controls the total abundances of sulphur species, as the other sulphur-bearing molecules are produced through chemistry from H_2S.

The abundances plotted in Fig. 2 are of two types: lower limits from rotation diagrams and strict lower limits where fewer than three transitions were available. The amount by which these column density lower limits underestimate the true abundances depends on unknowns such as the optical depth and temperature,

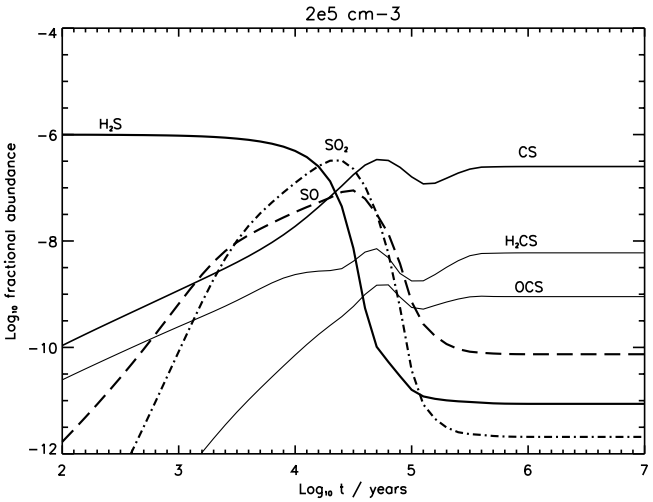

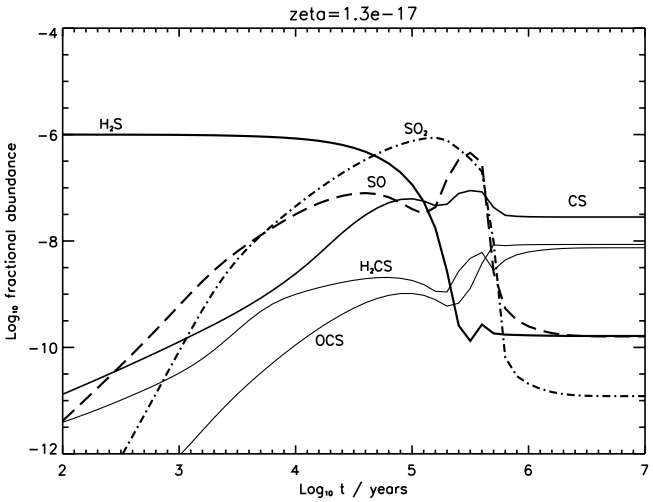

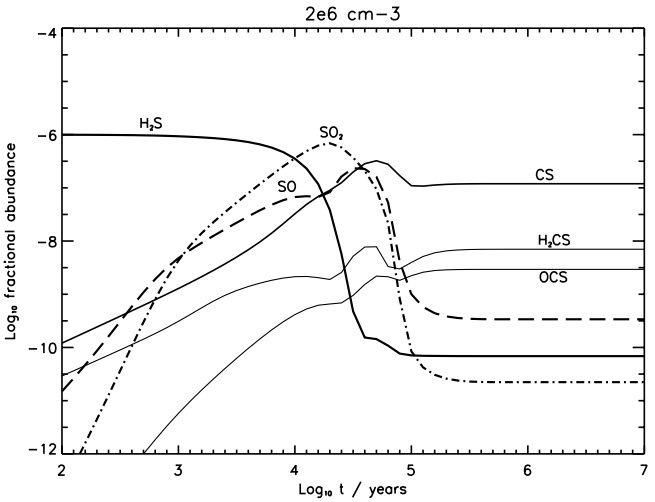

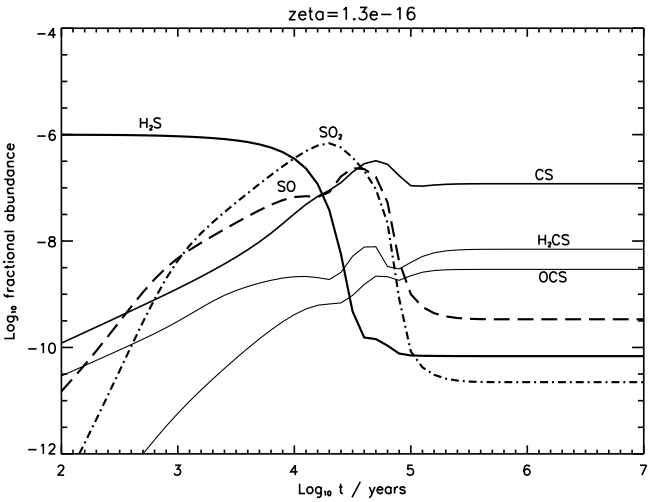

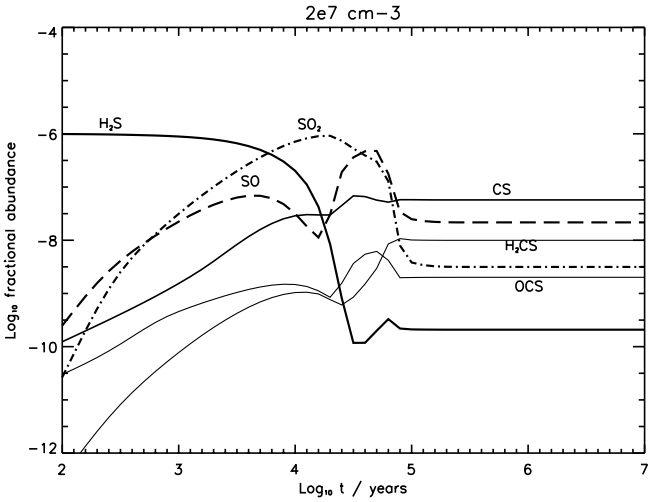

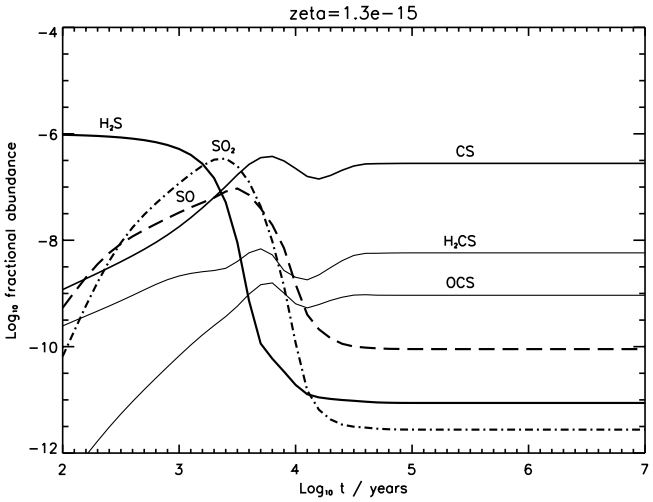

Fig. 5. Evolution of sulphur chemistry for different densities ($n_{\rm H_2} = 2 \times 10^5, 2 \times 10^6$ and 2×10^7 cm^{-3}) at a temperature of 100 K and cosmic ray rate of $\zeta = 1.2 \times 10^{-16}$ s^{-1}.

Fig. 6. Evolution of sulphur chemistry for different cosmic ray rates ($\zeta = 1.2 \times 10^{-17}, 1.2 \times 10^{-16}$ and 1.2×10^{-15} s^{-1} at a temperature of 100 K and a density of $n_{\rm H_2} = 2 \times 10^6$ cm^{-3}.

but by placing bounds on the likely range of these quantities, we can estimate by how much it would be possible to raise the abundances from the lower limits given while still remaining consistent with the observations. In addition, the size and location of the emission region affects the conversion from column density to abundance.

Optical depth gives us a clue as to the true column densities in SO and SO_2. Column densities of ^{32}SO and $^{32}SO_2$ estimated from ^{34}SO and $^{34}SO_2$, which we assume to be optically thin and rarer by a factor of 20 than their ^{32}S substituted variants, are given in Table 3. SO becomes optically thick at lower column densities than SO_2. The ^{32}SO column densities estimated from ^{34}SO are at most a factor of 2.5 greater than those estimated from ^{32}SO, indicating that optical depths in SO are small. The non-detection of $^{34}SO_2$ in most sources suggests that the optical depth in the $^{32}SO_2$ lines is also small. In G5.89 and G34.26, where $^{34}SO_2$ is detected, the increase in column density is a factor of 6 and 1.2 respectively. The ^{34}SO and $^{34}SO_2$ lines are weak and therefore abundances derived directly from these lines have large uncertainties, but they suggest that the true abundances of SO and SO_2 cannot exceed 10^{-7}.

For H_2S, the abundance lower limit is calculated on the basis of one observed transition with an excitation energy of 84 K, and the strict lower limit on the beam-averaged column density is given by calculating at a temperature of two-thirds of 84 K, or 56 K. If the true temperature were instead 20 K or 300 K, the H_2S line intensity would imply an H_2S abundance increased by a factor of 7–8. From a detection of $H_2^{34}S$ in G34.26, the optical depth in $H_2^{32}S$ is $\tau \sim 2$ which could approximately double the column density estimates.

Given these uncertainties, true abundances could be as much as 10^{-7} in H_2S and a few times 10^{-8} in SO_2 and SO. However, these abundances are still lower than are predicted by the models.

The models and observations can be reconciled if the initial abundance of H_2S released from the grain mantles were reduced from 10^{-6} to between 10^{-8} and 10^{-7}. The value of 10^{-6} was measured in the Orion Hot Core and Plateau regions by Minh et al. (1990). The initial abundance of H_2S in the hot core sources is limited by the highest abundance of H_2S, SO or SO_2 observed. Values from 10^{-8} to $\sim 10^{-7}$ would be consistent with the observations. This is consistent with an upper limit of 5×10^{-7} for the solid phase H_2S abundance towards W33A (Palumbo et al. 1997). With a better estimate of the temperature to use in the excitation calculation for H_2S, from further observations of H_2S and $H_2^{34}S$ lines, much of the remaining uncertainty in the initial H_2S abundance in these sources could be resolved.

A reduction in the initial H_2S abundance is not required if our assumption that the sizes and densities of the CH_3OH and sulphur species emission regions are similar is wrong. If the sulphur species were emitted from a smaller area than the CH_3OH then we would be counting hydrogen molecules from a larger region than sulphur species and underestimating abundances by a factor of (area of sulphur species emission) / (area of CH_3OH emission). However, the smaller region containing the sulphur species could not have the increase in hydrogen density usually associated with going to smaller size scales in hot cores, as this would cancel out the abundance advantage. The only way to reconcile the observed column densities of 10^{14}–10^{15} cm^{-2} with the abundances of 10^{-6} predicted by the models by adjusting sizes and densities is to release H_2S from grains only in a small fraction of the core or halo. This is possible but not consistent with a model in which the temperature and density increase towards the centre of the core and molecules are emitted from shells with appropriate excitation conditions.

Looking next at the H_2S-OCS problem, we see that in the models the abundances of H_2S and OCS only match at much lower abundances than H_2S, SO and SO_2. At times when H_2S, SO and SO_2 abundances are similar, abundances of OCS are predicted to be much less than H_2S, but are observed to be similar also. Abundances of OCS above those predicted by chemical models were also noted by Charnley (1997) in Sagittarius B2 and Orion, and OCS underproduction is a longstanding problem for gas phase chemical models. Charnley suggests that OCS is produced in grain mantles. OCS would then be evaporated along with H_2S and the other grain mantle species in these sources, and this could explain the high observed abundances. In support of this, the H_2S and OCS abundances appear to track each other from source to source. A weak infrared absorption near 4.9μm has been attributed to solid phase OCS: this has been detected towards W33A, AFGL 989 and Mon R2 IRS 2 (Palumbo et al. 1995, 1997). The calculated solid OCS abundances of 10^{-8}–10^{-7} are consistent with the observed gas phase abundances of 10^{-8}, so grains could be the source of all the OCS observed in the gas phase. However, it is hard to understand how OCS, which contains three heavy (non-hydrogen) atoms, can be formed on grains.

A revised chemical model with a reduced initial H_2S abundance of 10^{-8} in which both H_2S and OCS are initially injected into the gas phase is show in Fig. 7. This model can produce abundances of H_2S, OCS, SO_2 and CS within an order of magnitude of each other and consistent with the observed lower limits simultaneously at an age of 10^4 years (though as for the earlier models, the timescale depends heavily on the cosmic ray rate). The predicted SO abundance is lower than observed but the observed abundance may include a contribution from the halo. The time at which the H_2S and OCS abundances are equal depends on their starting abundances; if these are not equal, then the crossover is short, and more variation between sources would be expected.

H_2CS is also observed to have higher abundances than predicted by the model. In the models, at times when H_2S, SO and SO_2 abundances are similar, H_2CS abundances are two orders of magnitude less than the other sulphur species. Observed abundances in G9.62 and G34.26 are less than an order of magnitude less than H_2S and the CS:H_2CS ratio is no more than 30 in any source. H_2CS is produced from the reaction of atomic S and CH_3 or from electron recombination of H_3CS^+. H_2CS can become very abundant at high temperatures but only after substantial destruction of H_2S to provide atomic S (Charnley 1997).

Finally, we look for evidence of evolutionary differences between the cores. Evidence for evolution would show up in

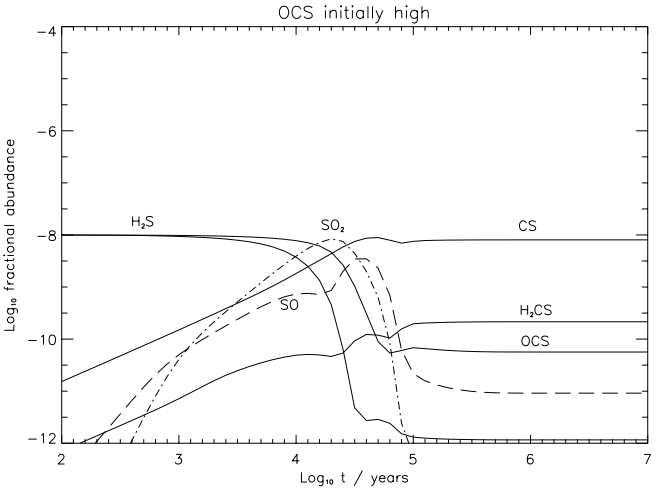

Fig. 7. Evolution of sulphur chemistry for an initial injection of both OCS and H_2S at abundances of 10^{-8}. The cosmic ray rate used was 1.2×10^{-16} s^{-1} at a temperature of 100 K and a density of $n_{\rm H_2} = 2 \times 10^6$ cm^{-3}.

Fig. 3 as differences in the relative abundances of species from source to source. The models show the relative abundances of species changing by several orders of magnitude over time, with H_2S surviving for $\sim 10^4$ years (depending on cosmic ray rate) and then being destroyed, SO and SO_2 rising gradually with time and then falling, and at later times CS, H_2CS and OCS dominating the chemistry. In younger cores, the models predict we should see H_2S and SO; at intermediate times, H_2S, SO and SO_2; later SO and SO_2 without H_2S; and finally, CS, OCS and H_2CS only (Millar et al. 1997; Charnley 1997).

In the data, however, relative abundances are similar in different sources (Fig. 3). H_2S varies by a factor of 7 between sources, H_2CS by a factor of 5 and OCS by a factor of 4. These variations are small and not what would be expected if the cores spanned a range of ages. On the basis of these similarities in abundances, the sources appear to be at similar evolutionary stages.

SO and SO_2 show slightly more variation than the other species with a factor of 10 difference between sources in SO and a factor of 20 in SO_2. The sources with high SO abundances also have high SO_2 abundances: these are G5.89, G75.78 and G10.47. This variation may be a result of small age differences between the sources, with higher SO and SO_2 abundances corresponding to older cores. In the models, SO and SO_2 abundances do not rise until after H_2S abundances have begun to fall. G75.78 also has a relatively low H_2S abundance, so H_2S may have begun to be destroyed in this source.

However, all three of the sources with high SO and SO_2 abundances – G5.89, G75.78 and G10.47 – are known to have molecular outflows. Shocks are predicted to produce large abundances of sulphur-bearing molecules in the gas phase (Pineau des Forêts et al. 1993) and high abundances have been observed in low mass outflows (eg. L1157, Bachiller et al. 1997). The high SO and SO_2 abundances in these sources may be a result of shock chemistry rather than hot core chemistry.

The seemingly similar ages of the cores, from the similar OCS, H_2S and H_2CS abundances, can be explained by selection effects. All the cores in our original survey were chosen on the basis of high excitation emission from ammonia (see the survey paper). The abundance of NH_3 is predicted by the chemical models to fall on a similar timescale to H_2S (Millar et al. 1997), so that older sources with low H_2S abundances would not be included in the sample. In addition, the sources from the survey for which we observed the most wavebands, and which are included in this study of sulphur species, were those that were strong emitters in CH_3CN (methyl cyanide). The chemistry of CH_3CN is not completely understood but models predict it to peak at times at which one would expect to observe H_2S, SO and SO_2 simultaneously. Hence the criteria by which the cores in this sample were selected, may have selected for cores with similar sulphur species abundances.

Quantitatively, the period in each model for which the H_2S, SO and SO_2 abundances are within an order of magnitude of each other is relatively short, and could be used to date the cores quite accurately if the physical conditions - and in particular the cosmic ray rate - were known. For the selection of models considered here, ages of a few thousand years up to 10^5 years are possible. Of the factors which remain uncertain and prevent us from from making more accurate estimates, temperature and density can be estimated from the excitation of the molecules, but the appropriate cosmic ray rate is very poorly known and has a strong effect on the timescales.

Also the cores must have a temperature/density gradient and the column densities include contributions from different regions along the line of sight. These gradients will shift the time where H_2S, SO and SO_2 can be observed simultaneously, as in the hotter parts of the core the chemistry will evolve more quickly compared to the cooler outer regions, and may be strong in SO and SO_2 while the outer parts of the core still contain H_2S. The shell model of G34.26 took this effect into account (Millar et al. 1997); with a better knowledge of source structure, this may be possible for more sources.

However, this upper limit of a few times 10^5 years is consistent with the observation of NH_3, CH_3OH and CH_3CCH in these cores. These species are destroyed in the hot, dense gas on similar timescales (Millar et al. 1997). It is also consistent with the estimated lifetimes of the nearby UC HII regions, $\sim 10^5$ years (Wood & Churchwell 1989).

4.1. Conclusions

We have compared the observed column densities of sulphur-bearing molecules – H_2S, SO, SO_2, OCS, CS and H_2CS – in eight sources with models of chemical evolution in hot cores. The abundances were calculated from observations with the JCMT, largely observed as part of our previously-published spectral line survey of molecular gas towards ultracompact HII regions (Hatchell et al. 1998b). The chemistry was based on that

used in our model of G34.26 (Millar et al. 1997) and the model of Charnley (1997).

- The models can produce the observed quantities of H_2S, SO, SO_2 and OCS for an initial abundance of H_2S of 10^{-8}–10^{-7}, lower by at least an order of magnitude than that measured in the Orion Hot Core by Minh et al. (1997).
- The models fail to predict abundances of 10^{-9}–10^{-8} for OCS and H_2S simultaneously. An alternative route to the formation of OCS, possibly grain chemistry, is required.
- The relative abundances of sulphur-bearing molecules vary little between sources, suggesting that the sources are at similar evolutionary stages. Age estimates lie between a few thousand and 10^5 years, but are heavily dependent on a knowledge of the cosmic ray rate.

We conclude that sulphur chemistry does have potential as a chemical clock, if the physical conditions of the region are well known. For most of the important species, column densities can be measured via millimetre/submillimetre line emission, and the chemistry (with the exception of OCS) is well understood. The accurate assignment of ages relies on a good knowledge of the cosmic ray rate, temperature, and (to a lesser extent) density: temperature and density can be estimated from the excitation of molecular lines, but lack of absolute knowledge of the cosmic ray rate makes it difficult to assign absolute ages to sources. However, sulphur chemistry should at least be valuable for assigning relative ages to sources in the same complex, where the same cosmic ray rate can be applied. Further work is required to determine the initial H_2S and OCS abundances injected from grains, and the rôle of shocks in hot cores.

Acknowledgements. This research was supported by the UK Particle Physics and Astronomy Research Council (PPARC) through grants to UMIST and the University of Kent. JH and MAT are grateful to PPARC for funding their postdoctoral position and studentship, respectively. The authors would like to thank the JCMT staff for their support during the observations, and S. Charnley for useful discussions.

References

Bachiller R., 1996, in E. F. van Dishoeck (Eds.) Molecules in Astrophysics (IAU 178) 103
Cesaroni R., Walmsley C. M., Churchwell E., 1992, A&A 256, 618
Charnley S. B., 1994, in 'Molecules and Grains and Space' ed. I. Nenner, pub. American Institute of Physics, p.155.
Charnley S. B., 1997, ApJ 481, 396
Churchwell E., Walmsley C. M., Cesaroni R., 1990, A&AS 83, 119
Hatchell, J., Millar, T. J., Rodgers, S. D., 1998a, A&A, 332, 695
Hatchell, J., Thompson, M. A., Millar, T. J., Macdonald, G. H., 1998b, A&AS, in press
Helmich F. P., Jansen D. J., de Graauw, Th., Groesbeck, T. D., van Dishoeck E. F., 1994, A&A 283, 626
Leen T. M., Graff M. M., 1988, ApJL, 325, 411
Macdonald G. H., Gibb A. G., Habing R. J., Millar T. J., 1996, A&AS 119, 333.
Millar T. J., Macdonald G. H., Gibb A. G., 1997, A&A, 325, 1163
Millar T. J., Macdonald G. H., Habing R. J., 1995, MNRAS 273, 25
Millar, T. J., Rawlings, J. M. C., Bennett, A., Brown, P. D., Charnley, S. B., 1991, Ap&SS, 87, 585
Minh Y. C., Ziurys L. M., Irvine W. M., McGonagle D., 1990, ApJ, 360, 136
Olmi L., Cesaroni R., Walmsley C. M., 1993, A&A 276, 489
Palumbo M. E., Tielens A. G. G. M., Tokunaga A. T., 1995, ApJ, 449, 674
Palumbo M. E., Geballe T. R., Tielens A. G. G. M., 1997, ApJ, 479, 839
Pineau des Forêts G., Roueff E., Schilke P., Flower D. R., 1993, MNRAS, 262, 915
Rodgers S. D., Millar T. J., 1996, MNRAS 280, 1046
Thompson, M. A., Macdonald, G. H., 1998, in preparation
Wood D. O. S., Churchwell E., 1989, ApJS, 69, 831
Yoshimura M., Koshi M., Matsui H., Kamiga K., Umeyama H., 1992, Chem.Phys.Lett. 189, 199